# The challenging conformational landscape of cysteamine···$H_2O$ revealed by the strong interplay of rotational spectroscopy and quantum chemical calculations

Wentao Song[1], Assimo Maris[1], Charlotte N. Cummings[2], Luca Evangelisti[1], Nicholas R. Walker[2] and Sonia Melandri[1]

[1] Dipartimento di Chimica "G. Ciamician", Università di Bologna, via F. Selmi 2, 40126, Bologna, Italy

[2] Chemistry- School of Natural and Environmental Sciences, Newcastle University, Bedson Building, Newcastle-upon-Tyne, NE1 7RU, U.K.

## Abstract

A 1:1 molecular complex of cysteamine with water is shown to adopt a cage-like structure where cysteamine accepts a relatively strong hydrogen bond from water while also engaging in two additional weaker interactions (SH···$O_w$ and CH···$O_w$). Experimental and theoretical approaches confirm this conformer as the global minimum on the potential energy surface. Fitting of key structural parameters to experimentally-determined moments of inertia yields consistent and accurate results for rotational and $^{14}N$ nuclear quadrupole coupling constants which are shown to be challenging to calculate using *ab initio* methods. Comprehensive analysis of the intermolecular interactions and a thorough comparison with the properties of aminoethanol-water is presented, utilizing independent gradient models based on Hirshfeld partition, quantum theory of atoms-in-molecules and symmetry-adapted perturbation theory approaches. As expected, the OH group of aminoethanol is a stronger hydrogen bond donor than the SH group in cysteamine, while the CH···$O_w$ interaction is a key determining factor of the conformational landscape in both cysteamine-water and aminoethanol-water complexes. The results show very clearly that the synergy between theoretical calculations and experimental results is not only desirable but mandatory to get the right answers in such complex conformational surfaces. The results are also a clear benchmark for the accuracy of different theoretical methods in assessing the structures and energy order of the conformations.

# Index

## Theoretical Methods

The Conformer-Rotamer Ensemble Sampling Tool (CREST) program was employed for conformational space exploration at the GFN2-xTB level of theory [1]. Geometry optimizations were performed using the GAUSSIAN 16 software (RevC.01 [2]) at the B3LYP-GD3(BJ)/def2-TZVP and MP2/aug-cc-pVTZ level of calculations. The symmetry-adapted perturbation theory (DF-SAPT2+(3)δMP2/aug-cc-pVTZ [3]) was applied using the Psi4 package [4] to calculate the intermolecular interaction energy values and derive the corresponding electrostatic, exchange, induction, and dispersion components. Electron density was analyzed utilizing both independent gradient models based on Hirshfeld (IGMH) partition [5] and the quantum theory of atoms-in-molecules (QTAIM [6]) as implemented in the Multiwfn program[7]. IGMH represents an advancement of the independent gradient model (IGM) [8–10]. In this approach, the free-state atomic densities implemented in the IGM method are replaced by atomic densities deduced from the real molecular electron density using Hirshfeld partition. SAPT, IGMH and QTAIM calculations where applied to the molecular complexes optimized at the MP2/aug-cc-pVTZ level of calculation.

## Experimental Methods

The experiment concerning CYS-W was conducted using two distinct spectrometers, namely the cavity-based Pulsed Jet Fourier Transform MicroWave (PJ-FTMW, 6 to 18 GHz) spectrometer at the University of Bologna, described elsewhere and updated with the FTMW++ set of programs [11–14], and the Chirped Pulse Fourier Transform Microwave (CP-FTMW, 6.5 to 18.5 GHz) spectrometer at the Newcastle University[15]. In the cavity-based PJ-FTMW spectrometer, Helium was passed over the $H_2O$ or $H_2{}^{18}O$ samples maintained at room temperature, with a backing pressure of $P_0$ (He) = 300 kPa, and then over CYS sample heated to $T$ = 320 K. The gaseous mixture was subsequently expanded into the Fabry-Pérot cavity through a solenoid valve (General Valve, Series 9, nozzle diameter 0.5 mm) to reach a pressure of approximately $10^{-3}$ Pa. The rotational temperature of the sample in the supersonic expansion was estimated to be around 2 K. Each rotational transition is split by the Doppler effect, due to the molecular beam expansion in the coaxial arrangement of the supersonic jet and resonator axes. The rest frequency is evaluated as the arithmetic mean of the frequencies of the Doppler components. The estimated accuracy of frequency measurements is better than 3 kHz and transitions separated by more than 7 kHz are resolvable. In the case of the CP-FTMW, a specialized nozzle furnished with a heating reservoir, was employed for the containment of the CYS sample. CYS was heated to 323 K, and argon, either mixed with $H_2O$ or $H_2{}^{18}O$ at room temperature, was utilized as a carrier gas to introduce it into the chamber. The pressure of argon was set to 300 kPa. In the frequency domain spectrum, an isolated line achieves a line width of 100 kHz, with an estimated accuracy of 10 kHz in the center frequencies of the lines at full width at half-maximum.

## Rotational spectra

The initial measurements on the complex were conducted employing the cavity-based PJ-FTMW spectrometer [11–14]. The focus was primarily on the two most stable conformers (#A and #B) but only one was observed. Given their high relative energies, it is anticipated that the majority of other conformers would exhibit relatively low populations within the context of our experimental setup.

The recorded rotational transitions displayed the hyperfine structure resulting from the nuclear quadrupole coupling (NQC) effect of the $^{14}$N atom, as illustrated in Figure 2(b) and (c). Observations included a total of 50 transitions comprising $\mu_a$, $\mu_b$ and $\mu_c$ R-type transition lines with $J'_{max}$=4, $K_a'_{max}$=2, $K_c'_{max}$=4. Moreover, the spectrum for the $^{34}$S isotopologue was observed in natural abundance (4.25%).

Complementary information was obtained using the broadband CP-FTMW spectrometer at the University of Newcastle[15]. Because of the lower spectral resolution, primarily attributed to the perpendicular alignment of the jet plume and the axis of radiation propagation, only a minor portion of the observed transitions showed a resolved, albeit only partly, nuclear hyperfine structure, and for these transitions in the majority of cases, we could discern only three lines of blended hyperfine components (two of them are shown in Figure 1(b) and (c)). Several μa, μb and μc R-type and μb Q-type transition lines were observed ($J'_{max}$=5, $K_a'_{max}$=4, $K_c'_{max}$=5) and 41 new transitions were identified.

Finally, using enriched $H_2{}^{18}O$, the $^{18}$O isotopologue of CYS-W was detected with both PJ-FTMW and CP-FTMW; a total of 15 lines was detected. The portion of the broadband spectrum recorded with the CP-FTMW spectrometer is reported in Figure 2.

## Cysteamine molecular structure

In order to obtain more information on the forces governing the structure of CYS and its complexes, we performed a structural fit on the five conformers of CYS monomer based on the experimental rotational constants reported by Song et. al.[16] and the equilibrium structures calculated at the MP2/aug-cc-pVTZ level (all data reported in Table S9).

By applying the procedure described in the previous section we could obtain the $r_e$ and $r_0$ parameters summarized in Tables S10-S13 of the supporting information.

The comparison of planar moment of inertia (Table S14) indicates that the experimental $M_{aa}$ values of all 5 observed conformers exceed the calculated ones by about 2 uÅ², while $M_{bb}$ and $M_{cc}$ of them have no significant changes, which means that the structure of the molecule is expanded along the *a*-axis direction compared to theoretical ($r_e$) structure. By comparison of the theoretical equilibrium structures, we can classify the structures according to the *trans* or *gauche* orientation of the amino group. Indeed, the $\alpha$(NCC) angle is significantly higher for Conf1-*gGt* and Conf5-*g'Gt* than Conf2-*gGg*, Conf3-*g'Gg* and Conf4-*g'Gg'* (116° vs 110°).
As concerns the structural changes upon water complexation, we compare the geometries of CYS Conf3-*g'Gg* and CYS-W Conf #A. It is worth noting that the $\alpha$(NCC) angle is expected to remain almost unchanged while structural fit suggests an increase of about 3.5°. The substantial disparity between the expected and observed values of the NQC constants can be attributed to this significant divergence.

Subsequently, we conducted a comparison between the experimental and theoretical monomer structures of AE. Upon analyzing the planar moment of inertia for both structures, we observed a phenomenon similar to that of CYS: the molecular skeleton exhibits a slight expansion along the *a*-axis compared to theoretical predictions.

## Tables

Table S1. Experimental transition frequencies ($\nu$), obs-calc. values ($\Delta\nu$) and the experimental accuracy of CYS-W.

| $J'$ | $K_a'$ | $K_c'$ | $F'$ | $J$ | $K_a$ | $K_c$ | $F$ | $\nu$ (MHz) | $\Delta\nu$(MHz) | *Err.* | $J'$ | $K_a'$ | $K_c'$ | $F'$ | $J$ | $K_a$ | $K_c$ | $F$ | $\nu$ (MHz) | $\Delta\nu$(MHz) | *Err.* |
|---|---|---|---|---|---|---|---|---|---|---|---|---|---|---|---|---|---|---|---|---|---|
| 2 | 0 | 2 | 2 | 1 | 0 | 1 | 2 | 8073.393 | 0.000 | 0.005 | 3 | 0 | 3 | 3 | 2 | 1 | 2 | 3 | 11112.087 | 0.001 | 0.005 |
| 2 | 0 | 2 | 2 | 1 | 0 | 1 | 1 | 8073.434 | 0.002 | 0.005 | 3 | 0 | 3 | 2 | 2 | 1 | 2 | 1 | 11112.337 | 0.000 | 0.005 |
| 2 | 0 | 2 | 3 | 1 | 0 | 1 | 2 | 8073.571 | 0.001 | 0.005 | 3 | 0 | 3 | 3 | 2 | 1 | 2 | 2 | 11112.368 | -0.004 | 0.005 |
| 2 | 0 | 2 | 1 | 1 | 0 | 1 | 0 | 8073.611 | 0.002 | 0.005 | 3 | 0 | 3 | 4 | 2 | 1 | 2 | 3 | 11112.391 | 0.001 | 0.005 |
| 2 | 0 | 2 | 1 | 1 | 0 | 1 | 1 | 8073.706 | -0.002 | 0.005 | 3 | 0 | 3 | 2 | 2 | 1 | 2 | 2 | 11112.783 | 0.001 | 0.005 |
| 2 | 1 | 2 | 3 | 1 | 1 | 1 | 2 | 7634.665 | -0.005 | 0.020 | 3 | 1 | 3 | 3 | 2 | 0 | 2 | 2 | 11739.200 | -0.002 | 0.005 |
| 2 | 1 | 1 | 1 | 1 | 1 | 0 | 1 | 9144.694 | 0.003 | 0.005 | 3 | 1 | 3 | 4 | 2 | 0 | 2 | 3 | 11739.367 | -0.001 | 0.005 |
| 2 | 1 | 1 | 2 | 1 | 1 | 0 | 1 | 9145.066 | -0.005 | 0.005 | 3 | 1 | 3 | 2 | 2 | 0 | 2 | 1 | 11739.395 | 0.005 | 0.005 |
| 2 | 1 | 1 | 3 | 1 | 1 | 0 | 2 | 9145.096 | 0.002 | 0.005 | 3 | 1 | 3 | 2 | 2 | 0 | 2 | 2 | 11739.661 | -0.004 | 0.005 |
| 2 | 1 | 1 | 1 | 1 | 1 | 0 | 0 | 9145.362 | 0.003 | 0.005 | 3 | 2 | 2 | 3 | 2 | 1 | 1 | 2 | 15272.193 | 0.007 | 0.020 |
| 2 | 1 | 2 | 2 | 1 | 0 | 1 | 2 | 8530.287 | 0.002 | 0.005 | 3 | 2 | 2 | 4 | 2 | 1 | 1 | 3 | 15272.427 | -0.003 | 0.020 |
| 2 | 1 | 2 | 2 | 1 | 0 | 1 | 1 | 8530.324 | 0.000 | 0.005 | 3 | 2 | 2 | 2 | 2 | 1 | 1 | 1 | 15272.575 | 0.010 | 0.020 |
| 2 | 1 | 2 | 3 | 1 | 0 | 1 | 2 | 8530.574 | 0.003 | 0.005 | 4 | 0 | 4 | 4 | 3 | 0 | 3 | 3 | 14940.153 | 0.051 | 0.020 |
| 2 | 1 | 2 | 1 | 1 | 0 | 1 | 0 | 8530.672 | 0.002 | 0.005 | 4 | 0 | 4 | 5 | 3 | 0 | 3 | 4 | 14940.153 | -0.028 | 0.020 |
| 2 | 1 | 2 | 1 | 1 | 0 | 1 | 1 | 8530.768 | -0.001 | 0.005 | 4 | 0 | 4 | 3 | 3 | 0 | 3 | 2 | 14940.153 | -0.020 | 0.020 |
| 2 | 1 | 1 | 1 | 1 | 0 | 1 | 0 | 10795.999 | 0.003 | 0.005 | 4 | 2 | 3 | 5 | 3 | 2 | 2 | 4 | 16522.221 | 0.020 | 0.020 |
| 2 | 1 | 1 | 1 | 1 | 0 | 1 | 1 | 10796.098 | 0.003 | 0.005 | 4 | 2 | 3 | 3 | 3 | 2 | 2 | 2 | 16522.221 | 0.006 | 0.020 |
| 2 | 1 | 1 | 3 | 1 | 0 | 1 | 2 | 10796.189 | -0.002 | 0.005 | 4 | 0 | 4 | 3 | 3 | 1 | 3 | 2 | 14770.170 | -0.011 | 0.020 |
| 2 | 1 | 1 | 2 | 1 | 0 | 1 | 2 | 10796.430 | -0.004 | 0.005 | 4 | 0 | 4 | 5 | 3 | 1 | 3 | 4 | 14770.170 | -0.033 | 0.020 |
| 2 | 1 | 1 | 2 | 1 | 0 | 1 | 1 | 10796.474 | 0.000 | 0.005 | 4 | 0 | 4 | 4 | 3 | 1 | 3 | 3 | 14770.170 | 0.006 | 0.020 |
| 2 | 2 | 1 | 2 | 1 | 1 | 0 | 1 | 11832.544 | 0.001 | 0.005 | 4 | 1 | 4 | 4 | 3 | 0 | 3 | 3 | 14992.047 | -0.002 | 0.005 |
| 2 | 2 | 1 | 3 | 1 | 1 | 0 | 2 | 11832.770 | 0.002 | 0.005 | 4 | 1 | 4 | 3 | 3 | 0 | 3 | 2 | 14992.136 | 0.002 | 0.005 |
| 2 | 2 | 1 | 1 | 1 | 1 | 0 | 0 | 11833.145 | 0.000 | 0.005 | 4 | 1 | 4 | 5 | 3 | 0 | 3 | 4 | 14992.136 | -0.003 | 0.005 |
| 2 | 2 | 0 | 1 | 1 | 1 | 1 | 0 | 12903.770 | -0.006 | 0.005 | 4 | 1 | 3 | 3 | 3 | 2 | 2 | 2 | 15551.218 | -0.003 | 0.005 |
| 2 | 2 | 0 | 3 | 1 | 1 | 1 | 2 | 12904.213 | -0.002 | 0.005 | 4 | 1 | 3 | 5 | 3 | 2 | 2 | 4 | 15551.239 | 0.002 | 0.005 |
| 2 | 2 | 0 | 1 | 1 | 1 | 1 | 1 | 12904.345 | 0.001 | 0.005 | 4 | 1 | 3 | 4 | 3 | 2 | 2 | 3 | 15551.299 | 0.002 | 0.005 |
| 2 | 2 | 0 | 2 | 1 | 1 | 1 | 2 | 12904.397 | 0.004 | 0.005 | 4 | 2 | 3 | 4 | 3 | 1 | 2 | 3 | 18338.519 | 0.008 | 0.020 |
| 2 | 2 | 0 | 2 | 1 | 1 | 1 | 1 | 12904.621 | 0.001 | 0.005 | 4 | 2 | 3 | 5 | 3 | 1 | 2 | 4 | 18338.772 | 0.032 | 0.020 |
| 3 | 0 | 3 | 3 | 2 | 0 | 2 | 3 | 11569.083 | -0.004 | 0.005 | 4 | 2 | 3 | 3 | 3 | 1 | 2 | 2 | 18338.772 | -0.043 | 0.020 |
| 3 | 0 | 3 | 3 | 2 | 0 | 2 | 2 | 11569.264 | 0.000 | 0.005 | 4 | 2 | 3 | 5 | 4 | 1 | 4 | 5 | 7955.699 | -0.024 | 0.020 |
| 3 | 0 | 3 | 4 | 2 | 0 | 2 | 3 | 11569.390 | 0.000 | 0.005 | 4 | 4 | 0 | 4 | 4 | 3 | 1 | 4 | 8009.922 | 0.011 | 0.020 |
| 3 | 0 | 3 | 2 | 2 | 0 | 2 | 2 | 11569.671 | -0.003 | 0.005 | 4 | 4 | 0 | 3 | 4 | 3 | 1 | 3 | 8010.024 | -0.005 | 0.020 |
| 3 | 1 | 3 | 2 | 2 | 1 | 2 | 1 | 11282.340 | 0.011 | 0.020 | 4 | 4 | 0 | 5 | 4 | 3 | 1 | 5 | 8010.024 | 0.019 | 0.020 |
| 3 | 1 | 3 | 3 | 2 | 1 | 2 | 2 | 11282.340 | 0.030 | 0.020 | 4 | 4 | 1 | 5 | 4 | 3 | 2 | 5 | 8554.494 | -0.017 | 0.020 |
| 3 | 1 | 3 | 4 | 2 | 1 | 2 | 3 | 11282.340 | -0.027 | 0.020 | 4 | 4 | 1 | 4 | 4 | 3 | 2 | 4 | 8554.494 | -0.026 | 0.020 |
| 3 | 1 | 2 | 3 | 2 | 1 | 1 | 2 | 13455.823 | 0.001 | 0.005 | 4 | 4 | 1 | 3 | 4 | 3 | 2 | 3 | 8554.494 | -0.015 | 0.020 |
| 3 | 1 | 2 | 4 | 2 | 1 | 1 | 3 | 13455.891 | 0.000 | 0.005 | 5 | 0 | 5 | 4 | 4 | 0 | 4 | 3 | 18337.379 | -0.008 | 0.020 |
| 3 | 1 | 2 | 2 | 2 | 1 | 1 | 1 | 13455.964 | -0.001 | 0.005 | 5 | 0 | 5 | 5 | 4 | 0 | 4 | 4 | 18337.379 | 0.029 | 0.020 |
| 3 | 1 | 2 | 3 | 2 | 1 | 1 | 3 | 13456.062 | -0.004 | 0.005 | 5 | 0 | 5 | 6 | 4 | 0 | 4 | 5 | 18337.379 | -0.019 | 0.020 |

| | | | | | | | | | | | | | | | | | | | | | |
|---|---|---|---|---|---|---|---|---|---|---|---|---|---|---|---|---|---|---|---|---|---|
| 3 | 2 | 1 | 4 | 2 | 2 | 0 | 3 | 13599.786 | 0.008 | 0.020 | 5 | 0 | 5 | 4 | 4 | 1 | 4 | 3 | 18285.452 | 0.025 | 0.020 |
| 3 | 2 | 1 | 2 | 2 | 2 | 0 | 1 | 13599.786 | 0.001 | 0.020 | 5 | 0 | 5 | 5 | 4 | 1 | 4 | 4 | 18285.452 | 0.049 | 0.020 |
| | | | | | | | | | | | 5 | 0 | 5 | 6 | 4 | 1 | 4 | 5 | 18285.452 | 0.012 | 0.020 |
| | | | | | | | | | | | 5 | 3 | 3 | 6 | 5 | 2 | 4 | 6 | 8398.277 | -0.011 | 0.020 |
| | | | | | | | | | | | 5 | 3 | 3 | 4 | 5 | 2 | 4 | 4 | 8398.277 | 0.027 | 0.020 |

Table S2. Experimental transition frequencies ($\nu$), obs-calc. values ($\Delta\nu$) and the experimental accuracy of the $^{18}$O and $^{34}$S isotopologue CYS-W.

**$^{18}$O**

| *J'* | $K_a'$ | $K_c'$ | *F'* | *J* | $K_a$ | $K_c$ | *F* | $\nu$(MHz) | $\Delta\nu$(MHz) | *Err.* | *J'* | $K_a'$ | $K_c'$ | *F'* | *J* | $K_a$ | $K_c$ | *F* | $\nu$(MHz) | $\Delta\nu$(MHz) | *Err.* |
|---|---|---|---|---|---|---|---|---|---|---|---|---|---|---|---|---|---|---|---|---|---|
| 2 | 0 | 2 | 2 | 1 | 0 | 1 | 2 | 7760.715 | -0.001 | 0.005 | 3 | 0 | 3 | 3 | 2 | 1 | 2 | 2 | 10641.147 | 0.003 | 0.005 |
| 2 | 0 | 2 | 2 | 1 | 0 | 1 | 1 | 7760.882 | -0.004 | 0.005 | 3 | 0 | 3 | 4 | 2 | 1 | 2 | 3 | 10641.212 | 0.004 | 0.005 |
| 2 | 0 | 2 | 3 | 1 | 0 | 1 | 2 | 7760.983 | -0.004 | 0.005 | 2 | 2 | 1 | 1 | 1 | 1 | 0 | 1 | 11554.955 | 0.007 | 0.005 |
| 2 | 0 | 2 | 1 | 1 | 0 | 1 | 1 | 7761.312 | 0.005 | 0.005 | 2 | 2 | 1 | 2 | 1 | 1 | 0 | 1 | 11555.233 | 0.001 | 0.005 |
| 2 | 1 | 2 | 2 | 1 | 0 | 1 | 2 | 8257.350 | -0.001 | 0.005 | 2 | 2 | 1 | 3 | 1 | 1 | 0 | 2 | 11555.336 | 0.004 | 0.005 |
| 2 | 1 | 2 | 2 | 1 | 0 | 1 | 1 | 8257.520 | -0.001 | 0.005 | 2 | 2 | 1 | 1 | 1 | 1 | 0 | 0 | 11555.652 | -0.002 | 0.005 |
| 2 | 1 | 2 | 3 | 1 | 0 | 1 | 2 | 8257.644 | -0.010 | 0.005 | 2 | 2 | 0 | 1 | 1 | 1 | 1 | 0 | 12557.676 | -0.002 | 0.005 |
| | | | | | | | | | | | 2 | 2 | 0 | 3 | 1 | 1 | 1 | 2 | 12557.994 | -0.003 | 0.005 |

**$^{34}$S**

| *J'* | $K_a'$ | $K_c'$ | *F'* | *J* | $K_a$ | $K_c$ | *F* | $\nu$(MHz) | $\Delta\nu$(MHz) | *Err.* | *J'* | $K_a'$ | $K_c'$ | *F'* | *J* | $K_a$ | $K_c$ | *F* | $\nu$ | $\Delta\nu$(MHz) | *Err.* |
|---|---|---|---|---|---|---|---|---|---|---|---|---|---|---|---|---|---|---|---|---|---|
| 2 | 1 | 2 | 2 | 1 | 0 | 1 | 1 | 8417.886 | 0.003 | 0.005 | 3 | 0 | 3 | 4 | 2 | 1 | 2 | 3 | 10902.630 | 0.002 | 0.005 |
| 2 | 1 | 2 | 3 | 1 | 0 | 1 | 2 | 8418.172 | -0.002 | 0.005 | 3 | 0 | 3 | 3 | 2 | 1 | 2 | 2 | 10902.630 | 0.000 | 0.005 |
| 2 | 0 | 2 | 2 | 1 | 0 | 1 | 1 | 7936.132 | 0.003 | 0.005 | 3 | 1 | 3 | 3 | 2 | 0 | 2 | 2 | 11570.104 | 0.000 | 0.005 |
| 2 | 0 | 2 | 3 | 1 | 0 | 1 | 2 | 7936.274 | -0.004 | 0.005 | 3 | 1 | 3 | 4 | 2 | 0 | 2 | 3 | 11570.296 | 0.000 | 0.005 |
| 2 | 2 | 0 | 3 | 1 | 1 | 1 | 2 | 12758.519 | -0.003 | 0.005 | | | | | | | | | | | |
| 2 | 2 | 0 | 2 | 1 | 1 | 1 | 1 | 12758.945 | 0.003 | 0.005 | | | | | | | | | | | |

Table S3. Comparison of spectroscopic parameters for CYS-W: theoretical (MP2/aug-cc-pVTZ), semiempirical (calculated from $r_0$) and experimental values.

| | Theoretical | Semiempirical | Experimental. | $\frac{(\text{Exp.}-\text{Theo})}{\text{Exp.}}$ | $\frac{(\text{Exp.}-\text{Semiemp.})}{\text{Exp.}}$ |
|---|---|---|---|---|---|
| *A*(MHz) | 3408.5978 | 3371.3468 | 3370.993(1) | -1.1% | 0.0% |
| *B*(MHz) | 2605.0957 | 2475.4091 | 2475.1442(8) | -5.3% | 0.0% |
| *C*(MHz) | 1802.7368 | 1719.8258 | 1719.8490(5) | -4.8% | 0.0% |
| $\chi_{aa}$(MHz) | 0.0760 | -0.1300 | -0.1311 | 158.0% | 0.9% |
| $\chi_{bb}$(MHz) | -1.0213 | -0.6783 | -0.7580 | -34.7% | 10.5% |
| $\chi_{cc}$(MHz) | 0.9452 | 0.8084 | 0.8891 | -6.3% | 9.1% |

Table S4. Experimental and theoretical (MP2/aug-cc-pVTZ) NQC constants (MHz) for CYS and AE.

| | Exp. | Theo. | Exp. | Theo. |
|---|---|---|---|---|
| | CYS-*g'Gg* [16] | CYS-*g'Gg* | AE-*g'Gg'* [17] | AE-*g'Gg'*. |
| $\chi_{aa}$ | 1.743(2) | 1.807 | -1.819(4) | 0.400 |
| $\chi_{bb}$ | 2.535(3) | 2.533 | 1.935(4) | -1.368 |
| $\chi_{cc}$ | -4.277(3) | -4.320 | -0.116(4) | 1.766 |

Table S5. Experimental spectroscopic parameters for CYS-W isotopologues (*S*-red, *I*r-rep.) and derived Kraitchman's substitution coordinates ($r_s$) of O and S atoms compared to the theoretical equilibrium values ($r_e$) and semi-experimental values ($r_0$).

| | CYS ($^{34}$S)-W | MP2($r_e$) | MP2($r_0$) | CYS-W($^{18}$O) | MP2($r_e$) | MP2($r_0$) |
|---|---|---|---|---|---|---|
| *A* (MHz) | 3344.90(2)[a] | 3387.23 | 3345.46 | 3301.0786(7) | 3328.23 | 3300.36 |
| *B* (MHz) | 2425.919(4) | 2549.49 | 2425.98 | 2370.567(2) | 2503.86 | 2370.35 |
| *C* (MHz) | 1691.0349(6) | 1772.13 | 1691.17 | 1652.1879(6) | 1733.44 | 1652.08 |
| $D_J$ (kHz) | [5.27][b] | | | [5.27] | | |
| $D_{JK}$ (kHz) | [-14.0] | | | [-14.0] | | |
| $D_K$ (kHz) | [16.3] | | | [16.3] | | |
| $d_1$ (kHz) | [2.05] | | | [2.05] | | |
| $1.5\chi_{aa}$ (MHz) | {0}[c] | 0.32 | 0.00 | -0.851(11) | -0.64 | -0.86 |
| $0.25(\chi_{bb}-\chi_{cc})$ (MHz) | -0.452(6) | -0.53 | -0.41 | -0.329(3) | 0.39 | -0.29 |
| $N$[d] | 10 | | | 15 | | |
| $\sigma$[e] (kHz) | 2.4 | | | 2.8 | | |
| *a* (Å) | ±1.415(1) | 1.425 | 1.415(6) | ±2.0711(7) | -2.011 | -2.071(4) |
| *b* (Å) | ±0.746(2) | -0.590 | 0.737(2) | ±1.354(1) | -1.198 | 1.358(3) |
| *c* (Å) | ±0.277(5) | -0.277 | -0.301(6) | ±0.212(7) | 0.219 | 0.250(3) |

[a]Standard errors in parentheses in units of the last digit; [b]Parameters in square brackets are fixed to the value of the parent species; [c]Parameters in curly brackets are fixed to 0; [d]Number of transitions in the fit; [e]Standard error deviation of the fit.

Table S6. Theoretical equilibrium structure ($r_e$) and fitted $r_0$ parameters of CYS-W.

| | | | | $r_e$ (MP2/aug-cc-pVTZ) | | | $r_0$ | | |
|---|---|---|---|---|---|---|---|---|---|
| | | | | $d_e$ [Å] | $\alpha_e$ [°] | $\tau_e$ [°] | $d_0$ [Å] | $\alpha_0$ [°] | $\tau_0$ [°] |
| C1 | N1 | | | 1.469 | | | | | |
| C2 | C1 | N1 | | 1.520 | 110.517 | | | **114(1)** | |
| S4 | C2 | C1 | N1 | 1.824 | 112.952 | 57.804 | | **112.4(8)** | |
| H1 | N1 | C1 | C2 | 1.013 | 110.069 | 172.669 | | | |
| H2 | N1 | H1 | C1 | 1.016 | 106.637 | -117.186 | | | |
| H3 | C1 | C2 | S4 | 1.095 | 109.178 | -66.333 | | | |
| H4 | C1 | C2 | S4 | 1.092 | 108.645 | 176.182 | | | |
| H5 | C2 | C1 | N1 | 1.089 | 109.769 | 176.277 | | | |
| H6 | C2 | C1 | N1 | 1.088 | 111.151 | -63.416 | | | |

| | | | | | | | | | |
|---|---|---|---|---|---|---|---|---|---|
| H7 | S4 | C2 | C1 | 1.340 | 95.332 | -89.347 | | | |
| O12 | S4 | C2 | C1 | 3.470 | 66.073 | -85.966 | **3.583(7)** | **68.0(7)** | **-82.8(9)** |
| H8 | O12 | S4 | C2 | 0.981 | 72.025 | 59.805 | | | |
| H9 | O12 | H8 | S4 | 0.961 | 105.576 | -157.270 | | | |

Table S7. Experimental and theoretical (MP2/aug-cc-pVTZ) spectroscopic parameters for AE-W.

| **EXP** | | **MEA-H2O-2**[17] | **MEA-H2O-1**[17] | **MEA-H2O-3**[17] |
|---|---|---|---|---|
| *A*/MHz | | 4886.463(2) | 4796.948(4) | 6154.586(1) |
| *B*/MHz | | 3356.059(2) | 3352.678(4) | 2322.1211(7) |
| *C*/MHz | | 2311.709(2) | 2132.416(3) | 2064.7071(6) |
| $\chi_{aa}$/MHz | | -1.819(4) | -2.175(5) | 0.842(3) |
| $\chi_{bb}$-$\chi_{cc}$/MHz | | 2.051(7) | -0.79(1) | 1.310(7) |
| **rDSD//B3** | | **Isomer 1**[17] | **Isomer 2**[17] | **Isomer 4**[17] |
| $A_0$/MHz | | 4882 | 4765 | 6104 |
| $B_0$/MHz | | 3334 | 3366 | 2307 |
| $C_0$/MHz | | 2281 | 2162 | 2052 |
| $\chi_{aa,0}$/MHz | | -1.609 | -2.318 | 0.825 |
| $\chi_{bb,0}$-$\chi_{cc,0}$/MHz | | 2.316 | -0.825 | 1.523 |
| **B3LYP-D3(BJ)/def2-TZVP** | **#A** | **Isomer 1**[17] | **Isomer 2**[17] | **Isomer 4**[17] |
| $A_e$/MHz | 4882.10 | 4915 | 4754 | 5888 |
| $B_e$/MHz | 3484.63 | 3444 | 3495 | 2458 |
| $C_e$/MHz | 2381.39 | 2337 | 2179 | 2153 |
| $\chi_{aa,e}$/MHz | -2.368 | -1.8 | -2.6 | 0.75 |
| $\chi_{bb,e}$-$\chi_{cc,e}$/MHz | 1.983 | 2.4 | -0.9 | 1.9 |
| $\Delta E_e$/kJ mol$^{-1}$ | 3.16 | 2.2 | 0 | 11.1 |
| $\Delta E_0$/MHz | 3.56 | 2.5 | 0 | 8.7 |
| **MP2/aug-cc-pVTZ** | **#A** | **#A'** | **#D** | **#E** |
| $A_e$/MHz | 4911.60 | 4989.87 | 4819.47 | 6023.39 |
| $B_e$/MHz | 3506.69 | 3435.52 | 3468.81 | 2493.80 |
| $C_e$/MHz | 2421.20 | 2357.10 | 2187.81 | 2194.33 |
| $\chi_{aa,e}$/MHz | -2.119 | -1.446 | -2.148 | 0.806 |
| $\chi_{bb,e}$-$\chi_{cc,e}$/MHz | 1.778 | 2.372 | -0.722 | 1.221 |
| $\Delta E_e$/MHz | 0 | 0.24 | 0.07 | 5.92 |

Table S8. Theoretical intermolecular binding and interaction energies (kJ·mol$^{-1}$) for CYS···W and the *g'Gg'*-AE···W.

| | CYS-W #A | CYS-W #B | CYS-W #C | CYS-W #D | AE-W #A | AE-W #A' | AE-W #D |
|---|---|---|---|---|---|---|---|
| $IE_{SAPT\Delta}$ | -43.3 | -39.5 | -35.0 | -36.7 | -52.5 | -51.5 | -51.5 |
| Electrostatic | -71.5 | -65.1 | -56.5 | -68.8 | -88.1 | -88.3 | -99.4 |
| Induction | -24.1 | -21.8 | -19.0 | -23.5 | -29.0 | -31.5 | -35.3 |
| Dispersion | -25.8 | -21.6 | -16.9 | -23.4 | -27.9 | -30.7 | -28.4 |

| | | | | | | | |
|---|---|---|---|---|---|---|---|
| Exchange-repulsion | 78.1 | 69.0 | 57.4 | 79.0 | 92.6 | 105.4 | 111.6 |

Table S9. Experimental and theoretical rotational constants (MHz) of the five observed conformers of CYS monomer.

| | | *A* | *B* | *C* |
|---|---|---|---|---|
| gGt | Calc | 11868.823 | 3347.1645 | 2897.0667 |
| | Exp | 11852.906 | 3310.634 | 2866.471 |
| | Exp-calc | -16 | -37 | -31 |
| | Exp-calc/Exp | -0.13% | -1.10% | -1.07% |
| gGg | Calc | 11996.155 | 3414.5397 | 2937.5716 |
| | Exp | 12008.0185 | 3363.5781 | 2898.8592 |
| | Exp-calc | 11.8635 | -50.9616 | -38.7124 |
| | Exp-calc/Exp | 0.10% | -1.52% | -1.34% |
| g'Gg | Calc | 11879.984 | 3465.371 | 2921.2263 |
| | Exp | 11932.433 | 3394.998 | 2877.8302 |
| | Exp-calc | 52.449 | -70.373 | -43.3961 |
| | Exp-calc/Exp | 0.44% | -2.07% | -1.51% |
| g'Gg' | Calc | 12015.301 | 3413.4884 | 2925.5367 |
| | Exp | 12042.9 | 3352.2284 | 2881.9906 |
| | Exp-calc | 27.599 | -61.26 | -43.5461 |
| | Exp-calc/Exp | 0.23% | -1.83% | -1.51% |
| g'Gt | Calc | 11919.841 | 3339.3105 | 2858.5937 |
| | Exp | 11944.628 | 3292.205 | 2827.008 |
| | Exp-calc | 24.787 | -47.1055 | -31.5857 |
| | Exp-calc/Exp | 0.21% | -1.43% | -1.12% |

Table S10. Theoretical equilibrium structure ($r_e$, MP2/aug-cc-pVTZ) and fitted $r_0$ parameters of CYS-*gGt*.

| | | | | $r_e$ | | | $r_0$ | | |
|---|---|---|---|---|---|---|---|---|---|
| | | | | $d_e$ [Å] | $\alpha_e$ [°] | $\tau_e$ [°] | $d_0$ [Å] | $\alpha_0$ [°] | $\tau_0$ [°] |
| N | | | | | | | | | |
| C1 | N | | | 1.455 | | | | | |
| C2 | C1 | N | | 1.527 | 115.882 | | | | |
| S | C2 | C1 | N | 1.821 | 113.190 | 59.910 | 1.8351(6) | 113.78(6) | 59.3(1) |
| H | N | C1 | C2 | 1.014 | 110.170 | 63.448 | | | |
| H | N | H | C1 | 1.015 | 106.531 | 118.455 | | | |
| H | C1 | C2 | S | 1.092 | 108.841 | -62.260 | | | |
| H | C1 | C2 | S | 1.092 | 108.429 | -178.159 | | | |
| H | C2 | C1 | N | 1.091 | 110.298 | -56.968 | | | |
| H | C2 | C1 | N | 1.090 | 111.273 | -176.656 | | | |
| H | S | C2 | C1 | 1.339 | 96.059 | 67.023 | | | |

Table S11. Theoretical equilibrium structure ($r_e$) and fitted $r_0$ parameters of CYS-gGg.

| | | | | $r_e$ (MP2/aug-cc-pVTZ) | | | $r_0$ | | |
|---|---|---|---|---|---|---|---|---|---|
| | | | | $d_e$ [Å] | $\alpha_e$ [°] | $d_e$ [Å] | $\alpha_e$ [°] | $d_e$ [Å] | $\alpha_e$ [°] |
| N | | | | | | | | | |
| C1 | N | | | 1.458 | | | 1.465(3) | | |
| C2 | C1 | N | | 1.518 | 109.835 | | 1.522(4) | 110.4(1) | |
| S | C2 | C1 | N | 1.822 | 113.080 | -63.033 | 1.826(3) | 113.6(1) | -63.0(1) |
| H | N | C1 | C2 | 1.012 | 110.703 | 179.533 | | | |
| H | N | H | C1 | 1.015 | 107.111 | 118.930 | | | |
| H | C1 | C2 | S | 1.092 | 108.281 | 178.951 | | | |
| H | C1 | C2 | S | 1.098 | 107.455 | 117.326 | | | |
| H | C2 | C1 | N | 1.090 | 109.639 | 53.503 | | | |
| H | C2 | C1 | N | 1.088 | 108.695 | -121.885 | | | |
| H | S | C2 | C1 | 1.339 | 96.069 | -68.208 | | | |

Table S12. Theoretical equilibrium structure ($r_e$) and fitted $r_0$ parameters of CYS-g'Gg.

| | | | | $r_e$ (MP2/aug-cc-pVTZ) | | | $r_0$ | | |
|---|---|---|---|---|---|---|---|---|---|
| | | | | $d_e$ [Å] | $\alpha_e$ [°] | $\tau_e$ [°] | $d_0$ [Å] | $\alpha_0$ [°] | $\tau_0$ [°] |
| N | | | | | | | | | |
| C1 | N | | | 1.461 | | | 1.465(3) | | |
| C2 | C1 | N | | 1.518 | 110.188 | | 1.525(4) | 110.5(2) | |
| S | C2 | C1 | N | 1.822 | 113.151 | -61.706 | 1.825(3) | 113.5(2) | 63.2(1) |
| H | N | C1 | C2 | 1.013 | 110.361 | -169.057 | | | |
| H | N | H | C1 | 1.014 | 106.421 | 118.471 | | | |
| H | C1 | C2 | S | 1.092 | 108.231 | -179.521 | | | |
| H | C1 | C2 | S | 1.096 | 107.788 | 117.592 | | | |
| H | C2 | C1 | N | 1.088 | 110.676 | 60.477 | | | |
| H | C2 | C1 | N | 1.090 | 108.630 | -121.361 | | | |
| H | S | C2 | C1 | 1.337 | 96.110 | 76.405 | | | |

Table S13. Theoretical equilibrium structure ($r_e$) and fitted $r_0$ parameters of CYS-g'Gg'.

| | | | | $r_e$ (MP2/aug-cc-pVTZ) | | | $r_0$ | | |
|---|---|---|---|---|---|---|---|---|---|
| | | | | $d_e$ [Å] | $\alpha_e$ [°] | $\tau_e$ [°] | $d_0$ [Å] | $\alpha_0$ [°] | $\tau_0$ [°] |
| N | | | | | | | | | |
| C1 | N | | | 1.463 | | | | | |
| C2 | C1 | N | | 1.520 | 109.950 | | | | |
| S | C2 | C1 | N | 1.818 | 112.548 | 63.953 | 1.834(7) | 113.9(7) | 63(1) |
| H | N | C1 | C2 | 1.012 | 110.802 | -168.261 | | | |
| H | N | H | C1 | 1.014 | 106.751 | 120.112 | | | |

| | | | | | | |
|---|---|---|---|---|---|---|
| H | C1 | C2 | S | 1.090 | 108.997 | -54.338 |
| H | C1 | C2 | S | 1.097 | 107.968 | 117.630 |
| H | C2 | C1 | N | 1.089 | 110.228 | -177.842 |
| H | C2 | C1 | N | 1.091 | 107.894 | -120.471 |
| H | S | C2 | C1 | 1.340 | 93.946 | -45.592 |

Table S14. Planar moment of inertia (uÅ$^2$) for five conformers of CYS, CYS-W, AE and AE-W.

| | $M_{aa}$ | | | $M_{bb}$ | | | $M_{cc}$ | | |
|---|---|---|---|---|---|---|---|---|---|
| | $r_e$ | $r_0$ | $r_0$- $r_e$ | $r_e$ | $r_0$ | $r_0$- $r_e$ | $r_e$ | $r_0$ | $r_0$- $r_e$ |
| gGt | 141.43 | 143.16 | 1.74 | 33.02 | 33.15 | 0.13 | 9.56 | 9.49 | -0.07 |
| gGg | 138.96 | 141.25 | 2.29 | 33.08 | 33.09 | 0.01 | 9.05 | 9.00 | -0.05 |
| g'Gg | 138.15 | 141.06 | 2.91 | 34.85 | 34.55 | -0.30 | 7.69 | 7.80 | 0.11 |
| g'Gg' | 139.37 | 142.08 | 2.71 | 33.38 | 33.28 | -0.10 | 8.68 | 8.68 | 0.00 |
| g'Gt | 142.87 | 144.98 | 2.11 | 33.92 | 33.79 | -0.14 | 8.47 | 8.52 | 0.05 |
| CYS-W | 163.0 | 174.1 | 11.02 | 117.3 | 119.8 | 2.49 | 31.0 | 30.1 | -0.83 |
| AE | 81.6 | 83.4 | 1.83 | 27.2 | 27.1 | -0.05 | 7.7 | 7.7 | -0.01 |
| AE-W | 135.9 | 132.9 | -3.01 | 95.1 | 85.7 | -9.37 | 9.8 | 17.7 | 7.90 |

**Figures**

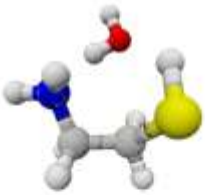

1
0 cm$^{-1}$
3375/2574/1775
3.4 D

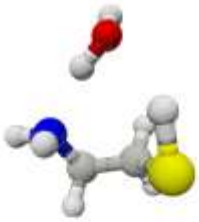

2
26 cm$^{-1}$
3306/2598/1734
3.6 D

3
152 cm$^{-1}$
4553/1778/1547
2.9 D

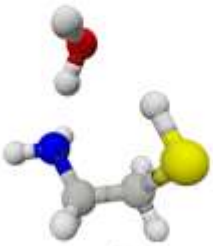

4
471 cm$^{-1}$
3214/2583/1524
4.0 D

5
535 cm$^{-1}$
8509/1158/1116
2.0 D

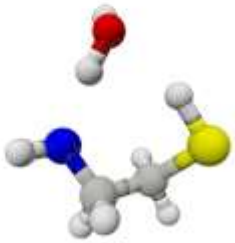

6
674 cm$^{-1}$
3196/2602/1532
4.8 D

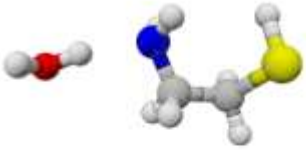

7
771 cm$^{-1}$
10609/1086/1035
2.1 D

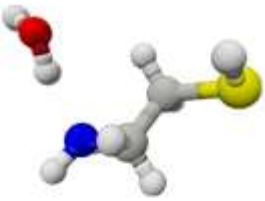

8
793 cm$^{-1}$
4952/1548/1258
3.4 D

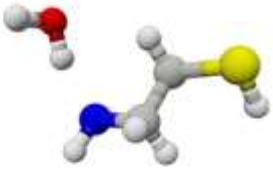

9
861 cm$^{-1}$
4967/1527/1229
4.1 D

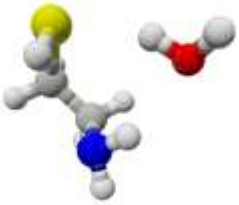

10
973 cm$^{-1}$
3188/2710/1692
0.4 D

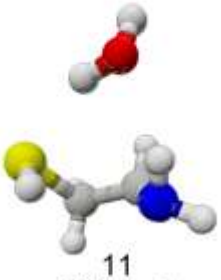

11
992 cm$^{-1}$
3167/2708/1668
2.4 D

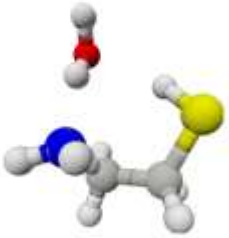

12
998 cm$^{-1}$
3448/2540/1685
3.3 D

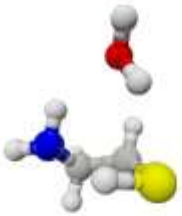

13
1154 $cm^{-1}$
3005/2820/1794
1.4 D

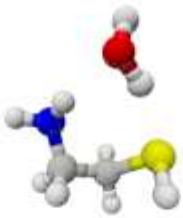

14
1209 $cm^{-1}$
3099/2626/1513
1.3 D

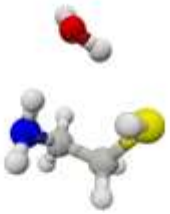

15
1248 $cm^{-1}$
3084/2707/1603
1.6 D

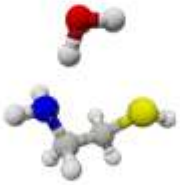

16
1357 $cm^{-1}$
3361/2436/1489
4.9 D

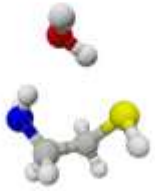

17
1381 $cm^{-1}$
3032/2637/1499
2.3 D

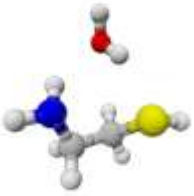

18
1462 $cm^{-1}$
3064/2800/1790
0.8 D

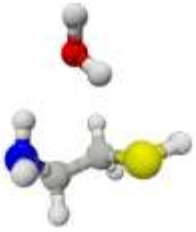

19
1500 $cm^{-1}$
2978/2805/1752
2.2 D

20
1515 $cm^{-1}$
2963/2780/1679
1.7 D

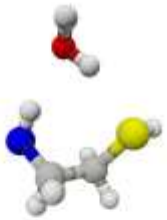

21
1696 $cm^{-1}$
3041/2653/1514
2.4 D

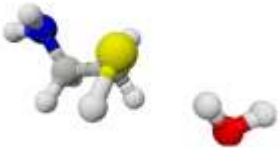

22
1699 $cm^{-1}$
6435/1442/1233
1.2 D

23
1707 $cm^{-1}$
6360/1438/1229
1.2 D

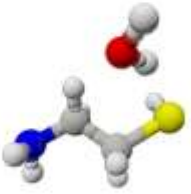

24
1745 $cm^{-1}$
3272/2163/1406
1.2 D

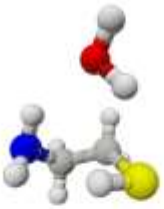

25
1761 $cm^{-1}$
2886/2786/1702
1.6 D

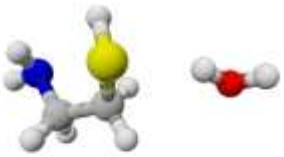

26
1796 $cm^{-1}$
5824/1468/1279
2.0 D

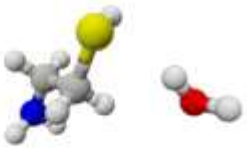

27
1851 $cm^{-1}$
4249/1539/1180
1.1 D

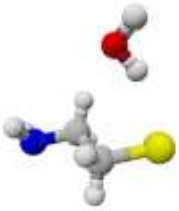

28
1912 $cm^{-1}$
3236/2163/1401
0.9 D

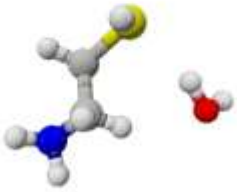

29
1920 $cm^{-1}$
3190/2054/1313
1.5 D

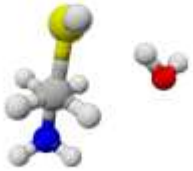

30
1926 $cm^{-1}$
3269/2162/1417
1.3 D

31
1988 $cm^{-1}$
3665/2060/1551
1.6 D

32
2080 $cm^{-1}$
4059/1915/1477
1.0 D

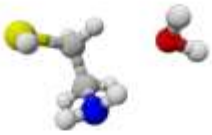

33
2195 $cm^{-1}$
4041/1671/1407
3.9 D

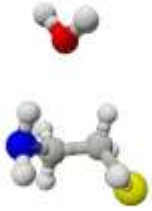

34
2196 $cm^{-1}$
3891/1727/1426
3.9 D

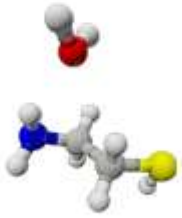

35
2278 $cm^{-1}$
4180/1601/1234
2.5 D

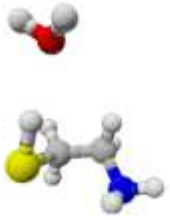

36
2411 $cm^{-1}$
3600/1760/1390
4.1 D

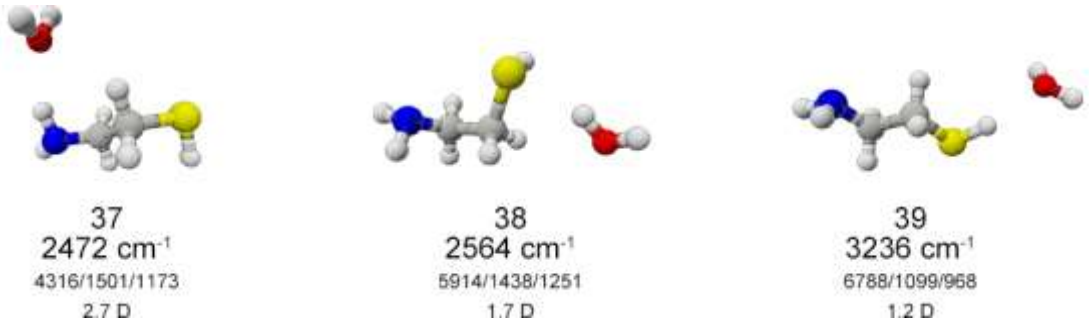


Figure S1. Structures, relative energies, rotational constants (*A/B/C* in MHz) and total dipole moments of the 39 non-equivalent conformers of cysteamine calculated at the B3LYP- GD3(BJ)/Def2TZVP level.

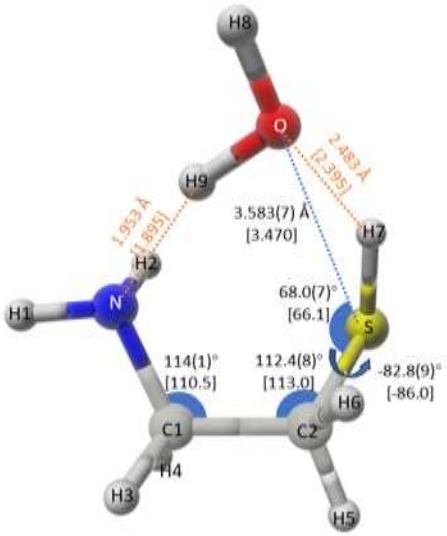


Figure S2. Structure of g'Gg-CYS-W (#A). The parameters of *ab initio* equilibrium structure $r_e$ are shown in square brackets and the parameters of pseudo-$r_0$ structure are shown without square brackets. The black values represent the fitted values and the orange values represent the derived values. Errors of fitted values are in parentheses. $r_e$ (CH-O)=2.541Å, pseudo-$r_0$(CH-O)=2.742 Å.

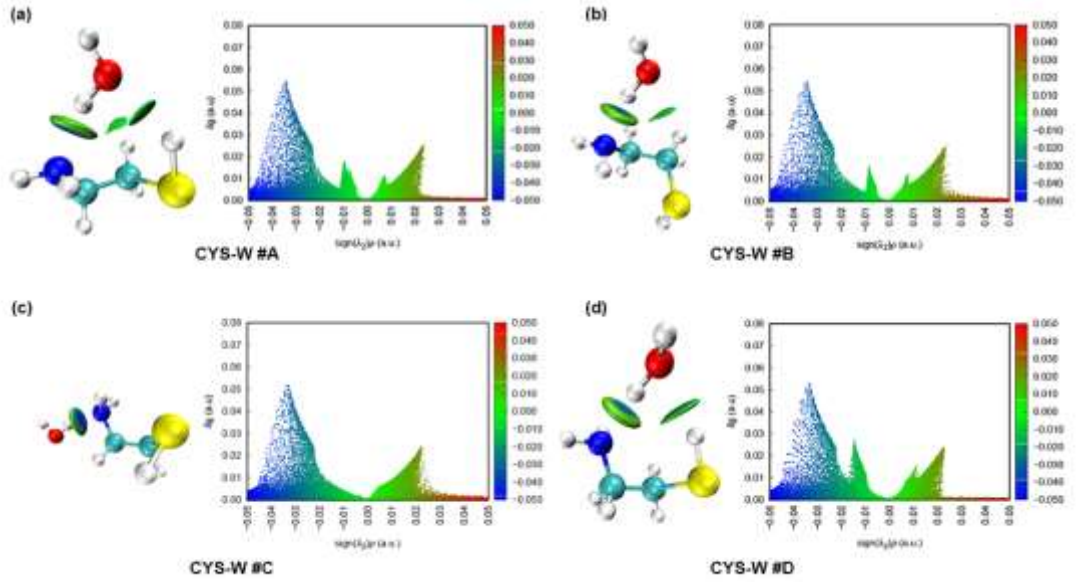


Figure S3. IGMH analysis results of the four most stable conformers of CYS-W. Three-dimensional isosurface and 2-D scatter plots. Isosurfaces are depicted at $\delta g$ isovalue of $\delta g = 0.01$ a.u. ($\delta g$ is a function of electron density gradient reflecting the interaction) and scatter plots are colored on a BGR scale corresponding to the $-0.05 < \text{sign}(\lambda_2)\ \rho < 0.05$ range. Essentially, IGMH employs the three-dimensional function to depict the interaction region between atoms.

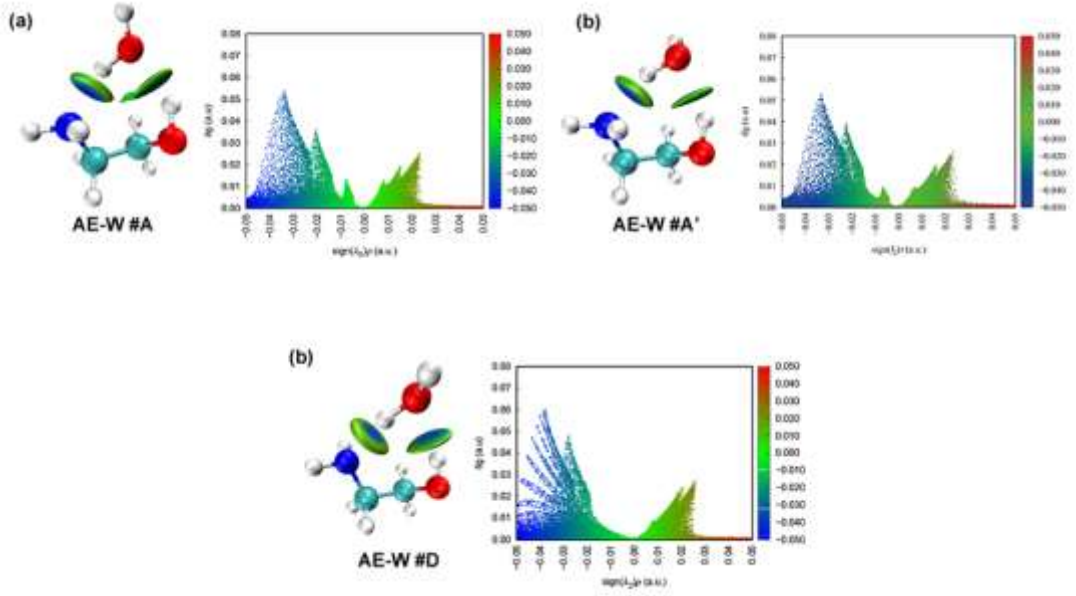


Figure S4. IGMH analysis results of AE-W #A (a), AE-W #A' (b) and AE-W #D (c). Three-dimensional isosurfaces and 2-D scatter plots. Three-dimensional isosurface and 2-D scatter plots. Isosurfaces are depicted at $\delta g$ isovalue of $\delta g = 0.01$ a.u. ($\delta g$ is a function of electron density gradient reflecting the interaction) and scatter plots are colored on a BGR scale corresponding to the $-0.05 < \text{sign}(\lambda_2)\ \rho < 0.05$ range. Essentially, IGMH employs the three-dimensional function to depict the interaction

region between atoms.

## References


(1) Pracht, P.; Bohle, F.; Grimme, S. Automated Exploration of the Low-Energy Chemical Space with Fast Quantum Chemical Methods. *Physical Chemistry Chemical Physics* **2020**, *22* (14), 7169–7192.

(2) Frisch, M. J.; Trucks, G. W.; Schlegel, H. B.; Scuseria, G. E.; Robb, M. A.; Cheeseman, J. R.; Scalmani, G.; Barone, V.; Petersson, G. A.; Nakatsuji, H.; Li, X.; Caricato, M.; Marenich, A. V; Bloino, J.; Janesko, B. G.; Gomperts, R.; Mennucci, B.; Hratchian, H. P.; Ortiz, J. V; Izmaylov, A. F.; Sonnenberg, J. L.; Williams-Young, D.; Ding, F.; Lipparini, F.; Egidi, F.; Goings, J.; Peng, B.; Petrone, A.; Henderson, T.; Ranasinghe, D.; Zakrzewski, V. G.; Gao, J.; Rega, N.; Zheng, G.; Liang, W.; Hada, M.; Ehara, M.; Toyota, K.; Fukuda, R.; Hasegawa, J.; Ishida, M.; Nakajima, T.; Honda, Y.; Kitao, O.; Nakai, H.; Vreven, T.; Throssell, K.; Montgomery Jr., J. A.; Peralta, J. E.; Ogliaro, F.; Bearpark, M. J.; Heyd, J. J.; Brothers, E. N.; Kudin, K. N.; Staroverov, V. N.; Keith, T. A.; Kobayashi, R.; Normand, J.; Raghavachari, K.; Rendell, A. P.; Burant, J. C.; Iyengar, S. S.; Tomasi, J.; Cossi, M.; Millam, J. M.; Klene, M.; Adamo, C.; Cammi, R.; Ochterski, J. W.; Martin, R. L.; Morokuma, K.; Farkas, O.; Foresman, J. B.; Fox, D. J. Gaussian˜16 Revision B.01. 2016.

(3) Jeziorski, B.; Moszynski, R.; Szalewicz, K. Perturbation Theory Approach to Intermolecular Potential Energy Surfaces of van Der Waals Complexes. *Chem Rev* **1994**, *94* (7), 1887–1930.

(4) Parrish, R. M.; Burns, L. A.; Smith, D. G. A.; Simmonett, A. C.; DePrince, A. E.; Hohenstein, E. G.; Bozkaya, U.; Sokolov, A. Y.; Di Remigio, R.; Richard, R. M.; Gonthier, J. F.; James, A. M.; McAlexander, H. R.; Kumar, A.; Saitow, M.; Wang, X.; Pritchard, B. P.; Verma, P.; Schaefer, H. F.; Patkowski, K.; King, R. A.; Valeev, E. F.; Evangelista, F. A.; Turney, J. M.; Crawford, T. D.; Sherrill, C. D. Psi4 1.1: An Open-Source Electronic Structure Program Emphasizing Automation, Advanced Libraries, and Interoperability. *J Chem Theory Comput* **2017**, *13* (7), 3185–3197.

(5) Lu, T.; Chen, Q. Independent Gradient Model Based on Hirshfeld Partition: A New Method for Visual Study of Interactions in Chemical Systems. *J Comput Chem* **2022**, *43* (8), 539–555.

(6) Bader, R. F. W. A Quantum Theory of Molecular Structure and Its Applications. *Chem Rev* **1991**, *91* (5), 893–928.

(7) Lu, T.; Chen, F. Multiwfn: A Multifunctional Wavefunction Analyzer. *J Comput Chem* **2012**, *33* (5), 580–592.

(8) Ponce-Vargas, M.; Lefebvre, C.; Boisson, J. C.; Hénon, E. Atomic Decomposition Scheme of Noncovalent Interactions Applied to Host-Guest Assemblies. *J Chem Inf Model* **2020**, *60* (1), 268–278.

(9) Lefebvre, C.; Rubez, G.; Khartabil, H.; Boisson, J. C.; Contreras-García, J.; Hénon, E. Accurately Extracting the Signature of Intermolecular Interactions Present in the NCI Plot of the Reduced Density Gradient versus Electron Density. *Physical Chemistry Chemical Physics* **2017**, *19* (27), 17928–17936.

(10) Lefebvre, C.; Khartabil, H.; Boisson, J. C.; Contreras-García, J.; Piquemal, J. P.; Hénon, E. The Independent Gradient Model: A New Approach for Probing Strong and Weak Interactions in Molecules from Wave Function Calculations. *ChemPhysChem* **2018**, *19* (6),

724–735. https://doi.org/10.1002/CPHC.201701325.

(11) Caminati, W.; Evangelisti, L.; Feng, G.; Giuliano, B. M.; Gou, Q.; Melandri, S.; Grabow, J.-U. On the Cl⋯ C Halogen Bond: A Rotational Study of CF 3 Cl–CO. *Physical Chemistry Chemical Physics* **2016**, *18* (27), 17851–17855.

(12) Caminati, W.; Millemaggi, A.; Alonso, J. L.; Lesarri, A.; López, J. C.; Mata, S. Molecular Beam Fourier Transform Microwave Spectrum of the Dimethylether–Xenon Complex: Tunnelling Splitting and 131Xe Quadrupole Coupling Constants. *Chem Phys Lett* **2004**, *392* (1–3), 1–6.

(13) Grabow, J.-U.; Stahl, W.; Dreizler, H. A Multioctave Coaxially Oriented Beam-Resonator Arrangement Fourier-Transform Microwave Spectrometer. *Review of scientific instruments* **1996**, *67* (12), 4072–4084.

(14) Balle, T. J.; Flygare, W. H. Fabry–Perot Cavity Pulsed Fourier Transform Microwave Spectrometer with a Pulsed Nozzle Particle Source. *Review of Scientific Instruments* **1981**, *52* (1), 33–45.

(15) Zaleski, D. P.; Stephens, S. L.; Walker, N. R. A Perspective on Chemistry in Transient Plasma from Broadband Rotational Spectroscopy. *Physical Chemistry Chemical Physics* **2014**, *16* (46), 25221–25228.

(16) Song, W.; Maris, A.; Rivilla, V. M.; Fortuna, F.; Evangelisti, L.; Lv, D.; Rodríguez-Almeida, L.; Jiménez-Serra, I.; Martín-Pintado, J.; Melandri, S. Micro-and Millimeter-Wave Spectra of Five Conformers of Cysteamine and Their Interstellar Search. *Astron Astrophys* **2022**, *661*, A129.

(17) Xie, F.; Mendolicchio, M.; Omarouayache, W.; Indira Murugachandran, S.; Lei, J.; Gou, Q.; Eugenia Sanz, M.; Barone, V.; Schnell, M. Structural and Electronic Evolution of Ethanolamine upon Microhydration: Insights from Hyperfine Resolved Rotational Spectroscopy. *Angewandte Chemie International Edition* **2024**, e202408622.